Flow management using natural instabilities*

J. M. FLORYAN

Department of Mechanical and Materials Engineering
The University of Western Ontario
London, Ontario, N5A 5B9, Canada

ACCIDENTAL INTRODUCTION of a small disturbance into an unstable flow leads to a large change in the form of the motion, e.g., laminar-turbulent transition. We wish to explore this phenomenon in the design of flow management strategies. We want to modulate the flow using a small input of external energy in such a way that the flow evolves through a natural instability process to a new, more desirable form. This presentation is focused on the use of distributed surface roughness for such purposes.

1. Introduction

WE WISH TO EXPLORE the use of surface roughness for modulation/rearrangements of different classes of flows. Our strategy relies on taking advantage of various instability mechanisms, so that the flow may evolve to a new form in a natural manner and this process can be started with only a small input of external energy. Success of this strategy relies on our understanding of the mechanisms driving the instability and the possible forms of the resulting motions. Different strategies may have to be developed depending on whether the drag reduction/increase, or increased/reduced mixing, or flow separation manipulation, or something else represent the main objective. Successful use of surface roughness for such purposes crucially depends on the understanding of the possible flow responses to various forms of the roughness.

Flows over rough walls have been studied since the early works of HAGEN [1] in 1854 and DARCY [2] in 1857, which were focused on turbulent regimes. REYNOLDS [3] was the first to pose the problem in the context of laminar-turbulent transition in 1883. The fundamental questions that were considered are: (i) what effects the distributed surface roughness can induce in a flow and (ii) when rough wall can be considered as being hydraulically smooth. While both questions are of considerable practical importance in several application areas, e.g. design of large Reynolds number laminar airfoils, small Reynolds nu-

---

*Paper presented at the 17–th Conference on Fluid Mechanics held in Bełchatów, September 17–21, 2006.

mber turbulent airfoils, compact heat exchangers, laminar electrostatic precipitators, etc., their rational resolution is still lacking.

The original investigations involved measurements of flows in open channels and in pipes. Various possible roughness forms were classified using the concept of "equivalent roughness" [4]. Phenomenological effects of the "equivalent roughness" were summarized in the form of friction coefficient [5–7]. These and other similar investigations show that surface roughness contributes directly to the dynamics of the flow only if the wall is hydraulically rough. The concept of hydraulic smoothness is conceptually very appealing, however no precise criterion exists that would allow predicting whether a given surface can be considered as being hydraulically smooth for the flow conditions of interest. While the modelling concepts of this type have been continuously re-evaluated [8, 9], they failed so far to uncover the mechanisms that govern the complex, flow-condition-dependent interaction between the roughness geometry and the moving fluid.

We shall now limit our discussion to the role played by roughness in the laminar-turbulent transition process. Experiments provide phenomenological description in the form of correlations between the height of the roughness, the flow conditions and the critical Reynolds number for certain classes of geometrical forms of the roughness [10–14]. The range of applicability of these correlations is not certain because they are based on limited experimental data and have been determined for, in essence, artificially created roughness forms. These correlations form a basis of all roughness-sensitive designs, nevertheless.

Generally speaking, the presence of roughness favors transition in the sense that under otherwise identical conditions, transition occurs at a lower Reynolds number on a rough wall rather than on a smooth wall. If the roughness height is sufficiently small, it has no effects on the transition process and the corresponding wall is considered to be hydraulically smooth. A frequently used criterion is that the roughness Reynolds number $\mathrm{Re}_k = U_k k/\nu < 25$ [15], where k is the roughness height, U_k is the undisturbed velocity at height k and ν the kinematic viscosity. Such a criterion does not address the issue of shape and distribution of the roughness.

The transition mechanisms activated by an isolated two-dimensional roughness, such as span-wise trip wire, are associated with inflectional separated velocity profiles and are considered to be understood at least on qualitative level [16]. Theoretical studies of such configurations lead to the determination of e^N transition criteria [17, 18]. The characteristic feature of the flow around an isolated, three-dimensional roughness element is the presence of the horseshoe vortex that generates streamwise vortices on the downstream side [15]. The mechanism governing transition is partially understood [15] and is thought to be associated with the strong instabilities of inflectional shear layers set up by the stream-

wise vortices, similarly as in the case of Görtler instability [19]. Experiments of RADEZTSKY *et al.* [20] indirectly confirm this view. The mechanisms associated with distributed surface roughness are not understood [15]. Various experiments indicate that when the roughness is operative, the departure from the laminar state is explosive [21, 22]. Past attempts to explain roughness effect in terms of Tollmien–Schlichting waves have failed [15, 22], however, more general recent formulations [23, 24] do show such a connection. Concepts based on the roughness-induced distortion of velocity profile proved to be inconclusive [25–27], similarly as the concepts based on the roughness-induced additional mixing [28]. Surface roughness may play a large role through amplification of the transient growth mechanism [29], however, this role remains to be substantiated. Surface vibrations provide additional complications [30].

Our interest is in the determination of the role played by distributed surface roughness in early stages of the transition process through the use of stability theory. One of the main conceptual difficulties arises in the context of modeling of the roughness geometry. The intuitive concept of surface roughness is well understood. One may touch a surface and decide (subjectively) if it is rough. The mathematical concept of rough surface is ill-defined, since infinitely many roughness forms are possible. It may appear that a general formulation is not possible and one must study roughness shapes on the case-by-case basis. This leads to a paradox, as it is not possible to investigate all possible shapes. This paradox is fictitious, however, since roughness geometry can be defined is some generality in the spectral space [23]. Analysis of the effects of different geometries is reduced in such formulation to scans of parameter space formed by the coefficients of spectral expansions. This concept has been utilized in the analysis of effects of distributed surface suction [23]. CABAL *et al.* [24] implemented it in the analysis of corrugation effects and provided a preliminary assessment of the effects of corrugation on flow instability.

The present discussion is carried out in the context of channel flow where one of the walls is rough. Presence of roughness may destabilize Tollmien–Schlichting waves [23, 24] as well as it may induce new forms of disturbances. The existing literature documents the existence of streamwise vortices in spatially periodic configurations. Such vortices may occur in the context of Langmuir circulation over surface waves [31, 32] where they are driven by the so-called CL1 and CL2 mechanisms. They may also occur in the flows over solid wavy walls [34–37] and in the flows modulated by suction [23], where centrifugal effect appears to be the dominant driving mechanism.

This presentation is organized as follows. Section 2 provides description of the flow in a rough channel. Section 3 summarizes linear stability analysis of this flow. Section 4 discusses selected results and shows where is the window of opportunity for flow re-arrangements.

2. Laminar flow in a channel with rough wall

In this section, we shall determine the form of the steady, two-dimensional flow in a channel with rough lower wall. This presentation is limited to a short outline, as details can be found in [23, 35]. We begin with the reference plane Poiseuille flow confined between flat rigid walls at $y = \pm 1$ and extending to infinity in the x-direction (Fig. 1). Velocity and pressure fields in the form

$$
\begin{aligned}
&\mathbf{V}_0(\mathbf{x}) = [u_0(x,y), v_0(x,y)] = [u_0(y), 0] = (1 - y^2,\ 0),\\
&p_0(\mathbf{x}) = -2\,x/\mathrm{Re}
\end{aligned}
$$

(2.1)

describe the fluid motion, where the motion is directed towards the positive x-axis and the Reynolds number Re is based on the half-channel height and the maximum x-velocity. Assume that the lower wall is replaced by a rough wall whose location $y_L(x)$ is specified as (see Fig. 1)

$$
(2.2) \qquad\qquad y_L(x) = -1 + \sum_{n=-\infty}^{n=\infty} S^{(n)} e^{in\alpha x},
$$

where $S^{(n)} = S^{(-n)*}$ and star denotes the complex conjugate. The wall is characterized by periodicity with the wavelength $\lambda = 2\pi/\alpha$, with the flow domain bounded by $-\infty < x < \infty$, $y_L(x) \le y \le 1$.
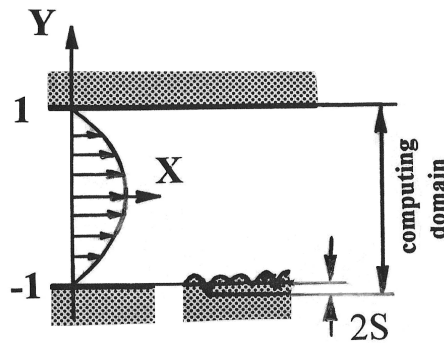
FIG. 1. Sketch of the flow domain.

The flow in the rough channel can be represented as

$$
\begin{aligned}
\mathbf{V}_2 &= [u(x,y), v(x,y)]\\
&= \mathbf{V}_0(x,y) + \mathbf{V}_1(x,y) = [u_0(y), 0] + [u_1(x,y), v_1(x,y)],\\[4pt]
p_2 &= p_0(x) + p_1(x,y),
\end{aligned}
$$

(2.3)

where $\mathbf{V}_1$ and p_1 are the velocity and pressure modifications due to the presence of the roughness. Substitution of the above representation of the flow quantities into the Navier–Stokes and continuity equations, introduction of the stream function defined as $u_1 = \partial_y \Psi, \; v_1 = -\partial_x \Psi$, elimination of pressure and representation of the unknowns in the form of Fourier expansions, e.g.,

$$\Psi(x,y) = \sum_{n=-\infty}^{n=+\infty} \Phi^{(n)}(y) e^{in\alpha x},$$

(2.4)
$$u_1(x,y) = \sum_{n=-\infty}^{n=+\infty} f_u^{(n)}(y)\, e^{in\alpha x},$$

$$v_1(x,y) = \sum_{n=-\infty}^{n=+\infty} f_v^{(n)}(y) e^{in\alpha x},$$

where $\Phi^{(n)} = \Phi^{(-n)^*}$, $f_u^{(n)} = f_u^{(-n)^*}$, $f_v^{(n)} = f_v^{(-n)^*}$, lead to a system of non-linear ordinary differential equations for the functions $\Phi^{(n)}$, $n \geq 0$, in the form

(2.5)
$$\left[D_n^2 - in\alpha \operatorname{Re}(u_0 D_n - D^2 u_0) \right] \Phi^{(n)}$$

$$- i\alpha \operatorname{Re} \sum_{k=-\infty}^{k=+\infty} \left[k\, D\Phi^{(n-k)} D_k \Phi^{(k)} - (n-k)\Phi^{(n-k)} D_k D\Phi^{(k)} \right] = 0 \, ,$$

where $D = d/dy$, $D_n = D^2 - n^2\alpha^2$. The boundary conditions at the channel walls are expressed in the form

(2.6)
$$u_0(y_L(x)) + u_1(x, y_L(x)) = 0, \qquad v_1(x, y_L(x)) = 0,$$
$$u_1(x,1) = 0, \qquad\qquad v_1(x,1) = 0.$$

The above formulation requires one arbitrary closing condition [23]. The reader may note that introduction of the roughness increases the resistance to the flow. Thus, if the flow is driven by the same mean pressure gradient, the volume flux has to decrease. Alternatively, if one wants to maintain the same volume flux, the mean pressure gradient must increase. All results presented in this paper have been obtained with the fixed volume flux condition.

The field equations have been solved using spectral methods based on the Chebyshev expansions. The boundary conditions on the smooth wall have been implemented using a variant of the tau technique [23], while the immersed boundary conditions method has been used to enforce the boundary conditions at the rough wall [38].

3. Linear stability

The natural change in the form of a flow begins with the growth of small disturbances. We wish to investigate how the introduction of distributed surface roughness can assist in promoting the growth of disturbances of desirable form and what is the required geometry of the roughness that is needed to promote such disturbances for the flow conditions of interest. The required information can be extracted with the help of the linear stability analysis of the roughness-modified flow.

Detailed description of the development of the linear stability equations for spatially modulated flows can be found in [23]. The following presentation is limited to a short outline. We begin with the governing equations in the form of vorticity transport and continuity equations. Unsteady, three-dimensional disturbances are superimposed on the mean part in the form

$$(3.1) \qquad \boldsymbol{\omega} = \boldsymbol{\omega}_2(x, y) + \boldsymbol{\omega}_3(x, y, z, t), \qquad \mathbf{V} = \mathbf{V}_2(x, y) + \mathbf{V}_3(x, y, z, t),$$

where subscripts 2 and 3 refer to the mean flow and the disturbance field, respectively. Equation (3.1) is substituted into the field equations, the mean part is subtracted and the equations are linearized. The resulting disturbance equations have the form

$$\nabla \cdot \mathbf{V}_3 = 0, \qquad \boldsymbol{\omega}_3 = \nabla \times \mathbf{V}_3,$$

$$(3.2)_1 \qquad \frac{\partial \boldsymbol{\omega}_3}{\partial t} + (\mathbf{V}_2 \cdot \nabla)\boldsymbol{\omega}_3 - (\boldsymbol{\omega}_3 \cdot \nabla)\mathbf{V}_2 + (\mathbf{V}_3 \cdot \nabla)\boldsymbol{\omega}_2$$

$$- (\boldsymbol{\omega}_2 \cdot \nabla)\mathbf{V}_3 = \mathrm{Re}^{-1}\nabla^2\boldsymbol{\omega}_3,$$

and are subject to the homogeneous boundary conditions

$$(3.2)_2 \qquad \mathbf{V}_3(x, 1, z, t) = 0, \qquad \mathbf{V}_3(x, y_L(x), z, t) = 0,$$

where y_L is given by Eq. (2.2). These boundary conditions are, in general, incomplete [39] and require an additional closing condition. All results presented in this paper have been obtained with the constant mass flux constraint.

Determination of the character of disturbance evolution requires solution of the initial value problem for Eqs. (3.2). The growth of disturbances, which is of interest for us, may have either a transient or a permanent character, depending on the flow conditions and the character of the initial disturbance field. This growth must be large enough to trigger nonlinear effects that are necessary in order to produce permanent change in the flow. The transient growth relies on the non-orthogonality between the modes resulting in a growth of a disturbance, even when all modes decay individually. This process always occurs in shear layers, but is relevant in the case of noisy environment where the initial

disturbance amplitudes are large enough so that the transient growth can reach the level necessary to trigger permanent change. One should note that the amplitudes and phases of the initial disturbances need to be adjusted properly in order to produce a significant transient effect. The permanent (or asymptotic) growth guarantees transition to a new state of the flow, but is more difficult to achieve since the required flow conditions are more restrictive as compared with the transient growth. The properly shaped surface roughness could be used to amplify transient growth and to expand the range of flow conditions that produce asymptotic growth. We begin the discussion with the asymptotic growth.

3.1. Asymptotic instability

In the case of asymptotic instability, the t and z dependence can be separated in the usual manner leading to the solution in the form

$$(3.3) \qquad \mathbf{v}_3(x, y, z, t) = [u_3(x, y), v_3(x, y), w_3(x, y)] \, e^{i(\delta x + \beta z - \sigma t)} + CC,$$

where δ and β are real and account for the streamwise and spanwise periodicity of the disturbance field, respectively. The exponent σ is complex and its imaginary and real parts describe the rate of growth and the frequency of disturbances, respectively, (u_3, v_3, w_3) stand for the amplitude of the disturbance velocity vector, and the eigenvalue problem for (δ, β, σ) for the corresponding partial differential equations can be easily derived. Rather than solving this problem numerically, we represent the disturbance amplitude in the form of Fourier expansions

$$u_3(x, y) = \sum_{m=-\infty}^{m=+\infty} g_u^{(m)}(y) e^{im\alpha x},$$

$$(3.4) \qquad v_3(x, y) = \sum_{m=-\infty}^{m=+\infty} g_v^{(m)}(y) e^{im\alpha x},$$

$$w_3(x, y) = \sum_{m=-\infty}^{m=+\infty} g_w^{(m)}(y) e^{im\alpha x}$$

leading to the final form of the disturbance velocity vector

$$(3.5) \qquad \mathbf{v}_3(x, y, z, t) = \sum_{m=-\infty}^{m=+\infty} \left[g_u^{(m)}(y), g_v^{(m)}(y), g_w^{(m)}(y) \right] e^{i[(\delta + m\alpha)x + \beta z - \sigma t]} + CC$$

and, eventually, to an eigenvalue problem for the ordinary differential equations describing functions $g_u^{(m)}, g_v^{(m)}, g_w^{(m)}$. Equation (3.3) may the viewed as the first step in the Fourier–Chebyshev method for the solution of the partial differential

equations for (u_3, v_3, w_3). Equation (3.5) provides a form of solution that is more convenient for the analysis.

Substitution of (3.5) into the disturbance Eqs. $(3.2)_1$ and separation of Fourier components result in a system of ordinary differential equations governing $g_u^{(m)}$, $g_v^{(m)}$, $g_w^{(m)}$ in the form

$$S^{(m)}\left(t_m g_w^{(m)} - \beta g_u^{(m)}\right) + C g_v^{(m)}$$

$$= i\text{Re} \sum_{n=-\infty}^{n=\infty} \left(W_u^{(m,n)} g_u^{(m-n)} + W_v^{(m,n)} g_v^{(m-n)} + W_w^{(m,n)} g_w^{(m-n)}\right),$$

(3.6)
$$T^{(m)} g_v^{(m)} = -R \sum_{n=-\infty}^{n=\infty} \left(B_u^{(m,n)} g_u^{(m-n)} + B_v^{(m,n)} g_v^{(m-n)} + B_w^{(m,n)} g_w^{(m-n)}\right),$$

$$it_m g_u^{(m)} + D g_v^{(m)} + i\beta g_w^{(m)} = 0,$$

where $-\infty < m+\infty$ and the explicit forms of the operators T, S, C, W, B are given in Appendix A. Operators S, C and T are referred to as the Squire [40] coupling and Orr–Sommerfeld operators [41, 42], respectively, due to their analogy with the similar operators in the smooth wall case [23].

The boundary conditions at the smooth wall can be set up in terms of individual modes, i.e.,

$$(3.7)_1 \qquad g_u^{(m)}(1) = g_v^{(m)}(1) = g_w^{(m)}(1) = 0, \qquad -\infty < m < +\infty$$

while boundary conditions at the rough wall involve complete modal functions, i.e.,

$$(3.7)_2 \qquad\qquad u_3(x, y_L(x)) = v_3(x, y_L(x)) = w_3(x, y_L(x)) = 0.$$

Equations (3.6) with boundary conditions (3.7) have nontrivial solutions only for certain combinations of parameters δ, σ and β. The required dispersion relation has to be determined numerically. For the purposes of calculations, the problem is posed as an eigenvalue problem for σ. Equations (3.6) are discretized with spectral accuracy using Chebyshev expansions. Boundary conditions at the upper wall are implemented using a version of the tau technique [23] while boundary conditions at the rough lower wall are implemented using the immersed boundary conditions concept [34].

The reader may note that the asymptotic analysis does not require the solution of an initial values problem. The information about the disturbance growth is deduced from an eigenvalue problem and negative values of the imaginary part of the complex growth rate σ identify growing disturbances as well as flow conditions when such growth is possible. One is interested in the determination of the changes in critical stability conditions induced by different forms of the roughness and in the form of disturbances that are most efficiently destabilized by the roughness.

3.2. Transient growth

In the case of asymptotic instability, the disturbances grow continuously in time. In general, disturbance may grow over a certain period of time even if all individual modes decay [47]. The maximum magnitude that the disturbances may achieve during transient growth could be sufficient to trigger transition to a new state. The analysis begins with the same formulation as used in the previous section. Details are given in [48]. The disturbances are assumed in the form

$$(3.8) \qquad \mathbf{v}_3(t, x, y, z) = [u_3(x, y, t), v_3(x, y, t), w_3(x, y, t)] e^{i(\delta x + \beta z)}$$

$$= \sum_{m=-\infty}^{m=+\infty} \left[g_u^{(m)}(t, y), g_v^{(m)}(t, y), g_w^{(m)}(t, y) \right] e^{i[(\delta + m\alpha)x + \beta z]} + CC$$

where β and δ are real and denote spanwise and streamwise wave numbers, respectively, and (u_3, v_3, w_3) stand for the disturbance amplitude modulated by the corrugation and being thus periodic in x. Equations (3.8) and (2.4) are substituted into (3.2) and re-arranged, and the Fourier modes are separated resulting in the following form of disturbances equations for $g_v^{(m)}$, $\theta^{(m)} = -\beta g_u^{(m)} + \gamma_m g_w^{(m)}$, i.e.,

$$(3.9)_1 \qquad \left(D^2 - k_m^2 \right) \partial_t g_v^{(m)}$$

$$- \operatorname{Re}^{-1} \left\{ \left(D^2 - k_m^2 \right)^2 - i \operatorname{Re} \gamma_m \left[u_0 \left(D^2 - k_m^2 \right) - D^2 u_0 \right] \right\} g_v^{(m)}$$

$$= \operatorname{Re}^{-1} \sum_{n=1}^{\infty} \left(\hat{G}_v^{(m,n)} g_v^{(m+n)} + G_v^{(m,n)} g_v^{(m-n)} \right.$$

$$\left. + \hat{G}_\theta^{(m,n)} \theta^{(m+n)} + G_\theta^{(m,n)} \theta^{(m-n)} \right) + G_v^{(0)} g_v^{(m)},$$

$(3.9)_2$ $\quad \partial_t \theta^{(m)} - \mathrm{Re}^{-1} \left[D^2 - k_m^2 - i\mathrm{Re}\,\gamma_m u_0 \right] \theta^{(m)} + \beta\, Du_0\, g_v^{(m)}$

$$= \mathrm{Re}^{-1} \sum_{n=1}^{\infty} \left(\hat{S}_v^{(m,n)} g_v^{(m+n)} + S_v^{(m,n)} g_v^{(m-n)} + \hat{S}_\theta^{(m,n)} \theta^{(m+n)} \right.$$

$$\left. + S_\theta^{(m,n)} \theta^{(m-n)} \right) + S_v^{(0)} g_v^{(m)} + S_\theta^{(0)} \theta^{(m)},$$

where $-\infty < m < +\infty$, $\gamma_m = \delta + m\alpha$. The explicit forms of the operators $G_v, G_\theta, \hat{G}_v, \hat{G}_\theta, S_v, S_\theta, \hat{S}_v, \hat{S}_\theta$ are given in the Appendix B. It can be shown that boundary conditions $(3.2)_2$ take the form analogous to (3.7), i.e.

$$u_3(x, y_L(x), t) = v_3(x, y_L(x), t) = w_3(x, y_L(x), t) = 0,$$

(3.10)

$$g_u^{(m)}(t, 1) = g_v^{(m)}(t, 1) = g_w^{(m)}(t, 1) = 0.$$

The boundary conditions at the upper wall are implemented using a version of the tau technique, while boundary conditions at the lower wall are implemented using the immersed boundary conditions concept.

Problem (3.9)–(3.10) has to be supplemented by initial conditions and thus one needs to consider all possible initial disturbances before making predictions regarding the growth process. This leads to an optimization problem where one seeks the form of disturbance leading to the largest possible growth at a given time, or the largest possible growth at all times, i.e., the optimal disturbance, as well as the magnitude of possible growth. The additional information that is being sought includes the identification of the form of the roughness that gives the largest possible transient growth, i.e. the optimal roughness.

4. Results and discussion

4.1. Traveling wave instability

The ideal Poiseuille flow (i.e. flow in a channel with smooth walls) becomes linearly unstable at $\mathrm{Re} = 5772.22$ and the critical disturbance has the form of a two-dimensional wave traveling in the streamwise direction with the wave number $\delta = 1.02$. Such waves are typically referred to as the Tollmien–Schlichting (TS) waves [43, 44]. We wish to determine how the presence of surface roughness affects the evolution of TS waves. Since roughness can have many forms, we illustrate the results with the simplest possible form, i.e, roughness in the form of a single Fourier harmonic. This shape provides a convenient reference point for studies of more complicated roughness shapes and is described by Eq. (2.2) with $S^{(1)} = S^{(-1)} = S$, $S^{(n)} = 0$ for $n \neq \pm 1$. The analysis is focused on the

asymptotic instability governed by the eigenvalues; issues related to transient growth are not addressed. The results presented are relevant to a flow system operating in a low-disturbance environment and have been obtained under the constant mass-flux constraint.

Variations of the amplification rate $\mathrm{Im}(\sigma)$ and frequency $\mathrm{Re}(\sigma)$ of disturbances as a function of the roughness wave number α and the disturbance wave number δ for the flow Reynolds $\mathrm{Re} = 6000$ and the roughness amplitude $S = 0.0085$ are displayed in Fig. 2. The same figure also shows the range of unstable disturbance wave numbers in the case of a smooth channel. It can be seen that presence of roughness leads to flow destabilization. Roughness with shorter wavelength is more effective, resulting in larger amplification rates as well as wider range of unstable δ. The frequency of disturbances appears to be not affected by the presence of roughness in the range of roughness wave numbers studied. Existence of such disturbances and the accuracy of theoretical predictions have been confirmed experimentally [45].
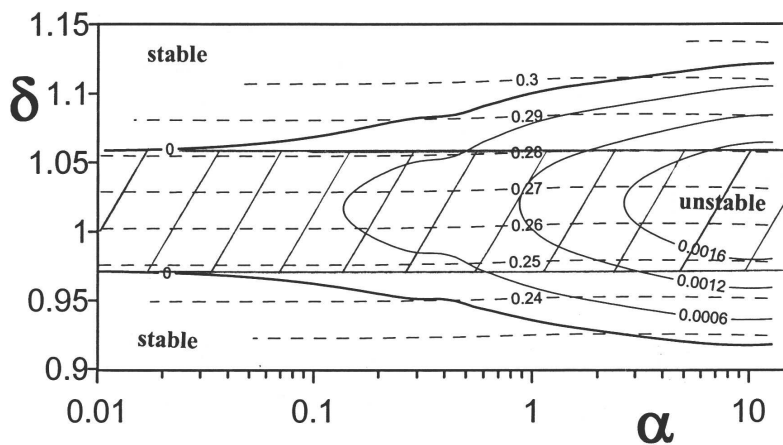
FIG. 2. Curves of constant amplification $\mathrm{Im}(\sigma)$ for the flow Reynolds number $\mathrm{Re} = 6000$ and the roughness amplitude $S = 0.0085$ as a function of the roughness wave number α and the disturbance wave number δ for the wavy wall roughness model. Dash lines correspond to $\mathrm{Re}(\sigma)$. Shaded area corresponds to the range of δ that is unstable in the case of smooth channel [39].

Variations of the neutral curves in the (α, δ) plane as a function of the flow Reynolds number Re for the roughness amplitude $S = 0.0085$ are illustrated in Fig. 3. It can be seen that the unstable disturbances can be found even at $\mathrm{Re} = 5000$, i.e., the presence of the roughness can significantly destabilize the flow. The two possible reasons for flow destabilization include changed vorticity dynamics associated with the formation of inflection points and the action of centrifugal forces. It may be not possible to separate these two effects. The
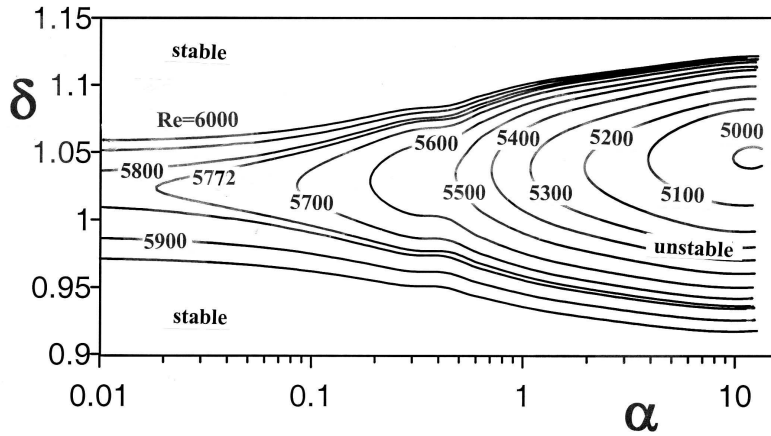
FIG. 3. Neutral curves for the roughness amplitude $S = 0.0085$ and for different values of the flow Reynolds number Re as a function of the roughness wave number α and the disturbance wave number δ for the wavy wall roughness model [39].
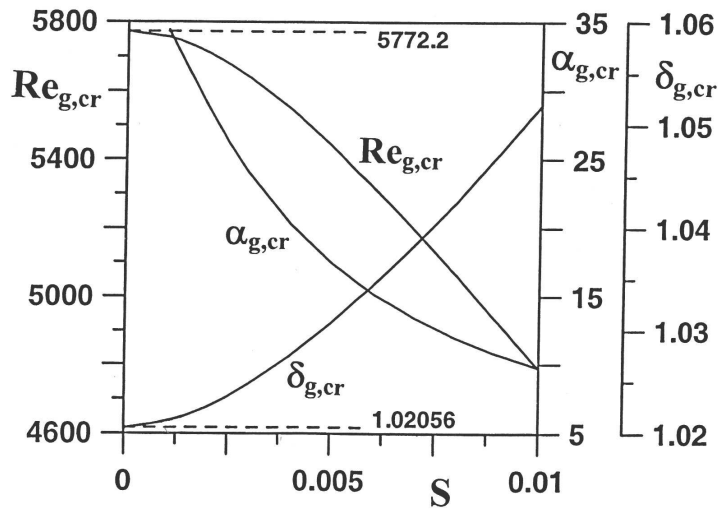
FIG. 4. The critical stability conditions for disturbances in the form of traveling waves for the wavy wall roughness model [39].

roughness ability to destabilize TS waves strongly depends on the roughness wave number α. We shall refer to the roughness wave numbers that destabilize the flow as the "active" wave numbers. The range of the "active" roughness wave numbers at Re = 5000 is rather small and concentrates around $\alpha \sim 10$. This

range rapidly expands in the direction of small and large α as Re increases to Re = 5000. Further increase of Re causes a very characteristic expansion in the direction of small α with the constant amplification curves forming a characteristic "bulge" pointing to the small-α direction. The case of Re = 5772 is of special interest. This value of Re corresponds to the critical Reynolds number in the case of smooth walls; the unstable zone shrinks to a single line $\delta(\alpha) = 1.02$ in the absence of roughness. Introduction of roughness expands this single line into a finite range of unstable δ for most of the range of the roughness wave numbers except for the roughness of sufficiently long wavelength, which actually stabilizes the flow. The stabilization in the case of Re = 5772 occurs for $\alpha < 0.02$. The stabilizing effect is rather weak; an increase of Reynolds number from Re = 5772 to Re = 5780 (not shown) extends the range of active α practically to $\alpha = 0$. Further increase of Re expands the range of unstable disturbance wave numbers δ and increases the amplification rates. It is worth pointing out that the maximum amplification always occurs at $\alpha \sim 10$ for this value of S.

Results discussed in the previous paragraphs permit identification of the critical stability conditions by carrying out studies similar to those illustrated in Figs. 2–3. It is convenient for presentation of the results to introduce a global critical Reynolds number $\mathrm{Re}_{g,cr}$ that defines the critical conditions for the onset of instability for a given roughness amplitude S regardless of its wave number α. Variations of the global critical conditions, including $\mathrm{Re}_{g,cr}$, the corresponding critical roughness wave number $\alpha_{g,cr}$ and the wave number of the critical disturbance $\delta_{g,cr}$ as a function of the roughness amplitude S are illustrated in Fig. 4. The area below the curve $\mathrm{Re}_{g,cr}(S)$ defines the flow the conditions and roughness geometry where roughness is not operative in the sense that it does not destabilize the traveling wave disturbances. The area above this curve defines flow conditions where there exists at least one active roughness wave number. The reader should note that the flow does not automatically become unstable for $\mathrm{Re} > \mathrm{Re}_{g,cr}$; the instability occurs if and only if the particular rough wall of interest contains an active roughness wave number.

4.2. Vortex instability

It has been determined that the presence of surface roughness gives rise to instability that results in the amplification of disturbances in the form of streamwise vortices. The amplification rates of such disturbances are illustrated in Fig. 5 for the flow Reynolds number Re = 5000 and the roughness amplitude $S = 0.0075$. It can be seen that the range of the "active" roughness wave numbers extends from $\alpha \approx 1.4$ to $\alpha \approx 7$. Each "active" roughness wave number gives

rise to a band of vortices whose wavelength is bounded from above and from below. The amplified vortex wave numbers are always contained in the interval $\sim 1.2 < \beta < \sim 3.7$ but the vortices that are actually amplified are contained in a smaller subinterval whose length and location change as a function of the roughness wave number. The magnitude of the amplification rate is similar to that found in the case of traveling waves.
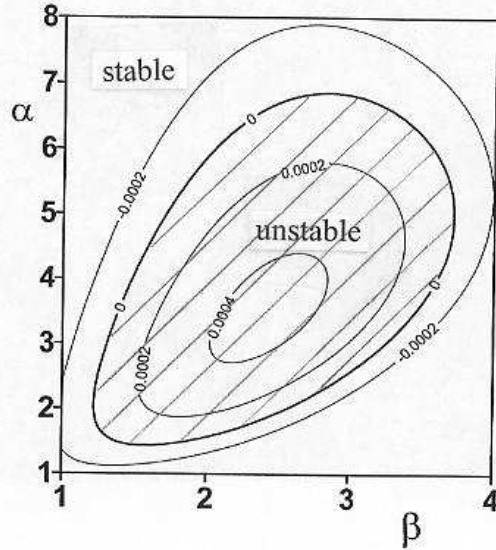
FIG. 5. Amplification rates $\text{Im}(\sigma)$ of disturbances in the form of streamwise vortices as a function of the roughness wave number α and the vortex wave number β for the flow Reynolds number $\text{Re} = 5000$ and the wavy-wall of amplitude $S = 0.0075$ [46].

The neutral surface in the $(\alpha, \beta, \text{Re})$ space for $S = 0.007$ is shown in Fig. 6. A rapid increase of the range of "active" roughness wave numbers α and the resulting vortex wave numbers β as Re increases is clearly visible. The tip of this surface identifies the global critical stability conditions, which are displayed in Fig. 7. The area below the critical curve defines the flow conditions when the roughness does not destabilize the vortex-like disturbances and is in this sense hydraulically "inactive", regardless of its wave number. The area above this curve defines the flow conditions where there exists at least one "active" roughness wave number. The flow does not automatically become unstable for $\text{Re} > \text{Re}_{g,cr}$; the instability occurs if and only if the particular rough wall contains an "active" roughness wave number.
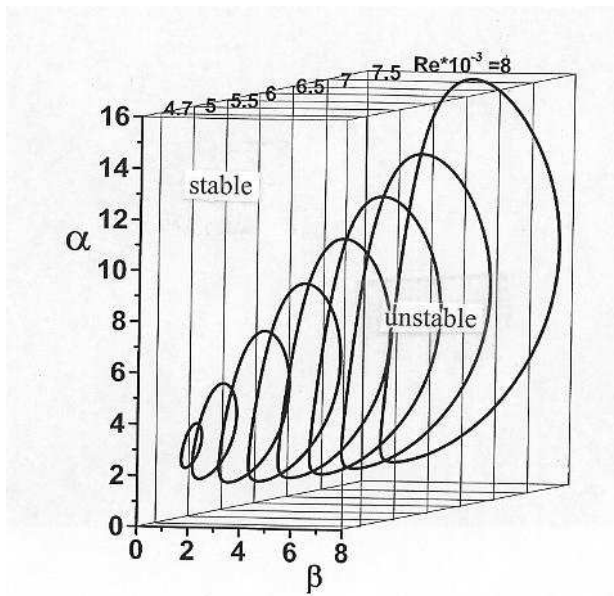
FIG. 6. The neutral surface describing instability giving rise to the vortex-like disturbances for the roughness amplitude $S = 0.007$ as a function of the flow Reynolds number Re, the roughness wave number α and the vortex wave number β for the wavy-wall roughness model [46].
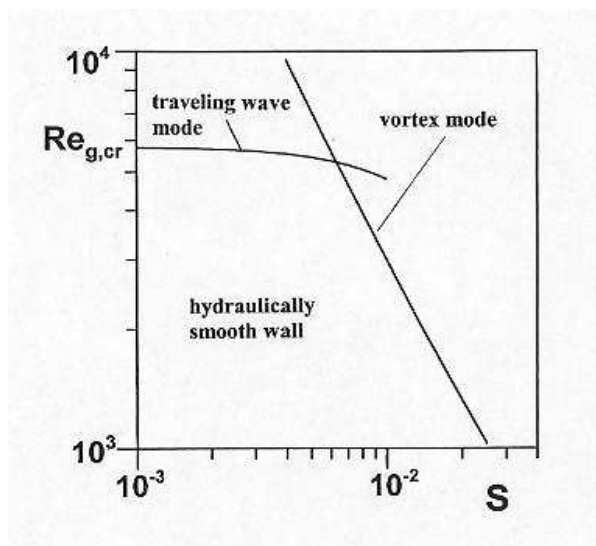
FIG. 7. Variations of the global critical Reynolds number $\mathrm{Re}_{g,cr}$ as a function of the roughness amplitude S for the wavy-wall roughness. The area below and to the left of both curves corresponds to the flow conditions and the wall geometry that do not produce any instability [46].

4.3. Global picture

The above discussion shows the existence of two independent modes of flow instability. One of our interests is in identifying the flow conditions where the flow is always stable, regardless of the form of the roughness and the type of instability. Since the critical roughness wavelength is very different at the onset for both modes, the general conclusion may be formulated without the need to consider interaction between both types of instability. The critical curves $\mathrm{Re}_{\mathrm{g,cr}}(S)$ for both instability modes are shown in Fig. 7 and permit identification of the flow conditions and wall geometry that do not produce any instability. Such a wall operating under the specified Reynolds number behaves as the hydraulically smooth wall. The opportunity for flow re-arrangements lies in the zone where the roughness is "active". The results shown in Fig. 7 identify the minimum roughness amplitude and the related shape that "activate" the roughness in the hydrodynamic sense.

4.4. Transient growth

Introduction of roughness with geometry identified in Fig. 7 gives rise to an instability that forces the flow to evolve to a new state. It is possible that the new state can be achieved with a subcritical roughness through the process of transient growth. The efficiency of the transient growth can be judged by identifying the maximum possible growth that can be achieved for the specified roughness geometry and the form of initial conditions that lead to this growth, i.e., the optimal disturbances. Repetition of such an analysis for different roughness forms leads to the identification of the optimal roughness, i.e., roughness form that is most efficient in the amplification of disturbances. Detailed analysis of this problem can be found in [48]. We wish now to focus on the interplay between the asymptotic instability and the transient growth and on the issue of manipulation of disturbance growth through change in the roughness amplitude. Transient growth for $\mathrm{Re} = 2000$, $\beta = 2$, $\delta = 0$, $\alpha = 3$ for different corrugation amplitudes S is illustrated in Fig. 8. In each case the initial conditions have been selected to maximize the growth at time $t = 50$. A very rapid initial growth always occurs regardless of the values of S. This growth eventually either disappears and disturbances decay for subcritical values of S, or asymptotic growth takes over and disturbances grow without limits for the supercritical values of S. Asymptotic growth leads to the vortex instability discussed in Sec. 4.2. Onset of transition requires activation of the nonlinear effects, which will certainly come into play in the case of modal instability. The transient growth is however so much stronger initially that it may decide on the fate of the flow even in the case of supercritical values of S. Results shown in Fig. 8 demonstrate that this

growth will amplify the disturbances by a factor of 500–1000 before asymptotic instability catches up. The same results also show that the roughness amplitude has to reach a certain critical magnitude to generate large growth. Once such an amplitude is achieved, the growth becomes very sensitive to any further very small changes in the roughness amplitude, which provides significant opportunities for the flow manipulation with very small changes of the controlling agent, i.e., the roughness size.
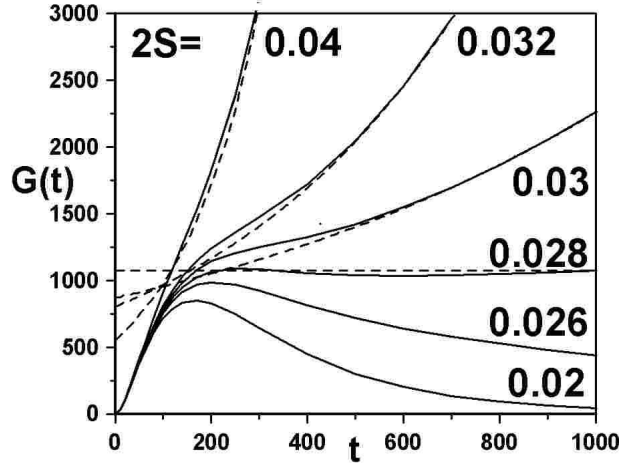
FIG. 8. Transient growth as a function of time for $Re = 2000$, $\beta = 2$, $\delta = 0$, $\alpha = 3$ for different values of the corrugation amplitude S. Initial conditions are selected in such a manner that the growth G at time $t = 50$ attains maximum for each S. Dash lines illustrate asymptotes defined by the asymptotic instability [48].

5. Summary

A significant improvement in the understanding of the role played by the surface roughness in the flow destabilization has been achieved. This knowledge forms the basis for the design of flow management strategies that utilize natural instabilities in the re-arrangement of fluid motions. The existing results identify the changes that can be induced in the flow through the intentional introduction of surface roughness and thus a design of surface roughness for flow management can be considered.

Acknowledgments

Appendix A.

Operators used in Eqs. (3.6) have the following definitions:

(A.1) $S^{(m)} = D^2 - k_m^2 - i\mathrm{Re}\,(t_m u_0 - \sigma)\,,$

(A.2) $T^{(m)} = \left(D^2 - k_m^2\right)^2 - i\mathrm{Re}\left[(t_m u_0 - \sigma)(D^2 - k_m^2) - t_m D^2 u_0\right],$

(A.3) $C = \mathrm{Re}\beta D u_0,$

(A.4) $W_u^{(m,n)} = \beta(i f_v^{(n)} D - t_m f_u^{(n)}),$

(A.5) $W_v^{(m,n)} = i\beta D f_u^{(n)},$

(A.6) $W_w^{(m,n)} = t_m(t_{m-n} f_u^{(n)} - i f_v^{(n)} D),$

(A.7) $B_u^{(m,n)} = -t_m^2 D f_u^{(n)}$
$$+ in\alpha k_m^2 f_v^{(n)} - t_m^2 f_u^{(n)} D + it_m D f_u^{(n)} D + it_m f_v^{(n)} D^2,$$

(A.8) $B_w^{(m,n)} = \beta\left(- t_{m-2n} f_u^{(n)} D - t_{m-n} D f_u^{(n)} + i f_v^{(n)} D^2\right),$

(A.9) $B_v^{(m,n)} = i k_m^2 t_{m-n} f_u^{(n)} + k_m^2 D f_v^{(n)}$
$$+ k_m^2 f_v^{(n)} D + it_m D^2 f_u^{(n)} + it_m D f_u^{(n)} D,$$

where $D = d/dy$, $t_m = m\alpha + \delta$ and $k_m^2 = t_m^2 + \beta^2$.

Appendix B.

Operators used in Eqs. $(3.9)_1$–$(3.9)_2$ are defined as follows:

(B.1) $G_v^{(m,n)} = \mathrm{Re}\left[\dfrac{i\,n\alpha}{k_{m-n}^2}\left(\beta^2 - \gamma_m \gamma_{m-n}\right) D f_u^{(n)} D\right.$

$$+ \dfrac{k_m^2}{k_{m-n}}^2 \left(\beta^2 + \gamma_{m-n}\gamma_{m-2n}\right) f_v^{(n)} D + \dfrac{i}{k_{m-n}^2}\left(2n\alpha\beta^2 - \gamma_m k_{m-n}^2\right) f_u^{(n)} D^2$$

$$\left. + \dfrac{i}{k_{m-n}^2}\left(n\alpha\gamma_m - k_m^2\right) f_v^{(n)} D^3 + i\,k_m^2 \gamma_{m-2n} f_u^{(n)} + i\,\gamma_m D^2 f_u^{(n)}\right],$$

$$(B.2) \qquad \hat{G}_v^{(m,n)} = \mathrm{Re} \left[\frac{i\,n\alpha}{k_{m+n}^2} \left(\gamma_m \gamma_{m+n} - \beta^2 \right) \left(D f_u^{(n)} \right)^* D \right.$$

$$+ \frac{k_m^2}{k_{m+n}^2} \left(\beta^2 + \gamma_{m+n} \gamma_{m+2n} \right) \left(f_v^{(n)} \right)^* D$$

$$+ \frac{i}{k_{m+n}^2} \left(-2n\alpha\beta^2 - \gamma_m k_{m+n}^2 \right) \left(f_u^{(n)} \right)^* D^2$$

$$+ \frac{i}{k_{m+n}^2} \left(-n\alpha\gamma_m - k_m^2 \right) \left(f_v^{(n)} \right)^* D^3$$

$$\left. + i\,k_m^2 \gamma_{m+2n} \left(f_u^{(n)} \right)^* + i\,\gamma_m \left(D^2 f_u^{(n)} \right)^* \right],$$

$$(B.3) \qquad G_v^{(0)} = -i\gamma_m [f_u^{(0)}(D^2 - k_m^{(2)}) - D^2 f_u^{(0)}],$$

$$(B.4) \qquad \hat{S}_\theta^{(m,n)} = \mathrm{Re} \left[-i\gamma_m \left(f_u^{(m)} \right)^* - \frac{1}{k_{m+n}^2} \left(\beta^2 + \gamma_m \gamma_{m+n} \right) \left(f_v^{(n)} \right)^* D \right],$$

$$(B.5) \qquad S_\theta^{(0)} = -i\gamma_m f_u^{(0)},$$

$$(B.6) \qquad S_v^{(0)} = -\beta D f_u^{(0)},$$

$$(B.7) \qquad S_v^{(m,n)} = \mathrm{Re} \left[\beta\, D f_u^{(n)} - \frac{in\alpha\beta}{k_{m-n}^2} f_v^{(n)} D^2 \right],$$

$$(B.8) \qquad \hat{S}_v^{(m,n)} = \mathrm{Re} \left[\beta \left(D f_u^{(n)} \right)^* + \frac{in\alpha\beta}{k_{m+n}^2} \left(f_v^{(n)} \right)^* D^2 \right],$$

$$(B.9) \qquad S_\theta^{(m,n)} = \mathrm{Re} \left[-i\gamma_m f_u^{(m)} - \frac{1}{k_{m-n}^2} \left(\beta^2 + \gamma_m \gamma_{m-n} \right) f_v^{(n)} D \right],$$

$$(B.10) \qquad G_\theta^{(m,n)} = \mathrm{Re} \left[\frac{1}{k_{m-n}^2} 2n\alpha\beta\gamma_{m-n} f_u^{(n)} D + \frac{n\alpha\beta}{k_{m-n}^2} \left(\gamma_m + \gamma_{m-n} \right) D f_u^{(n)} \right.$$

$$\left. - \frac{in\alpha\beta k_m^2}{k_{m-n}^2} f_v^{(n)} - \frac{in\alpha\beta}{k_{m-n}^2} f_v^{(n)} D^2 \right],$$

$$(B.11) \qquad \hat{G}_\theta^{(m,n)} = \mathrm{Re} \left[-\frac{1}{k_{m+n}^2} 2n\alpha\beta\gamma_{m+n} \left(f_u^{(n)} \right)^* D \right.$$

$$\left. - \frac{n\alpha\beta}{k_{m+n}^2} \left(\gamma_m + \gamma_{m+n} \right) \left(D f_u^{(n)} \right)^* + \frac{in\alpha\beta k_m^2}{k_{m+n}^2} \left(f_v^{(n)} \right)^* + \frac{in\alpha\beta}{k_{m+n}^2} \left(f_v^{(n)} \right)^* D^2 \right].$$

References

1. G. Hagen, *Uber den Einfluss der Temperatur auf die Bewegung des Wasser in Röhren*, Math. Abh. Akad. Wiss., 17–98, Berlin 1854.

2. H. Darcy, *Recherches expérimentales relatives au mouvement de l'eau dans les tuyaux*, Mallet-Bachelier, Paris 1857.

3. O. Reynolds, *An experimental investigation of the circumstances which determine whether the motion of water shall be direct or sinuous, and of the wall of resistance in parallel channels*, Philos. Trans. R. Soc. London, **174**, 935, 1883.

4. J. Jimenez, *Turbulent flows over rough walls*, Ann. Rev. Fluid Mech., 173–196, 2004.

5. J. Nikuradse, *Strömungsgesetze in Rauhen Rohren,* VDI-Forschungscheft #36, 1933, (also NACA TM 1292, 1950).

6. C. F. Colebrook, *Turbulent flow in pipes, with particular reference to the transition region between smooth and rough pipes,* J. Inst. Civ, Eng., **11**, 133, 1939.

7. L. F. Moody, *Friction factors for pipe flow,* Transactions of the ASME, **66**, 671, 1944.

8. P. Bradshaw, *A note on "critical roughness" and "transitional roughness"*, Phys. Fluids, **12**, 1611, 2000.

9. D. R. Waigh and R. Kind, *Improved aerodynamic characterization of regular three-dimensional roughness,* AIAA J. **36**, 1117, 1998.

10. A. Fage, *The smallest size of span wise surface corrugation which affects boundary layer transition on an airfoil,* Br. Aero. Res. Council Report No. 2120, 1943.

11. B. H. Carmichael, *Surface waviness criteria for swept and unswept laminar suction wings*, Northrop Aircraft Report No. NOR-59-438 (BLC123), 1957.

12. H. Schlichting, *Boundary layer theory*, 7-th ed., McGraw–Hill, 1979.

13. I. Tani, *Effect of two dimensional and isolated roughness elements*, [in:] *Boundary Layer and Flow Control*, G. V. Lachman [Ed.], Pergamon, **2,** 637, 1961.

14. A. E. Doenhoff and A. L. Braslow, *The effect of distributed surface roughness on laminar airfoil*, [in:] *Boundary Layer and Flow Control*, G.V. Lachman [Ed.], Pergamon, **2**, 657, 1961.

15. M. V. Morkovin, *On roughness-induced transition: facts, views and speculations*, [in:] *Instability and Transition*, M.Y. Hussaini and R.G. Voigt [Eds.], **1**, 281, ICASE/NASA LARC Series, Springer 1990.

16. P. S. Klebanoff and K. D. Tidstrom, *Mechanism by which a two-dimensional roughness element induces boundary layer transition,* Phys. Fluids **15**, 1172, 1972.

17. A. H. Nayfeh, S. A. Ragab and A. A. Al-Maaitah, *Effect of bulges on the stability of boundary layers,* Phys.Fluids, **4**, 796, 1988.

18. J. A. Masad and V. Iyer, *Transition prediction and control in subsonic flow over a hump,* Phys. Fluids, **6**, 313, 1994.

19. J. M. Floryan, *On the Görtler instability of boundary layers,* Progress in Aerospace Sciences, **28**, 235, 1991.

20. R. H. Radeztsky, M. S. Reibert and W. S. Saric, *Effect of isolated micron-sized roughness on transition in swept-wing flows,* AIAA J., **37**, 1370, 1999.

21. E. Reshotko, *Disturbances in a laminar boundary layer due to distributed surface roughness* [in:] *Turbulence and Chaotic Phenomena,* T. Tatsumi [Ed.] Proceedings of IUTAM Symposium, 39, 1984, Elsevier.

22. T. C. Corke, A. Bar Sever and M. V. Morkovin, *Experiments on transition enhancements by distributed roughness,* Phys. Fluids, **29**, 3199, 1986.

23. J. M. Floryan, *Stability of wall-bounded shear layers in the presence of simulated distributed roughness,* J. Fluid Mech., **335**, 29, 1997.

24. T. Cabal, J. Szumbarski and J. M. Floryan, *Stability of flow in a wavy channel,* J. Fluid Mech., **457**, 191, 2002.

25. K. Sing and J. L. Lumley, *Effect of roughness on the velocity profile of a laminar boundary layer,* Appl. Sci. Res., **24**, 168, 1972.

26. M. Lessen and S. T. Gangwani, *Effect of small amplitude wall waviness upon the stability of the laminar boundary layer,* Phys. Fluids, **19**, 510, 1976.

27. J. M. Kendall, *Laminar boundary layer velocity distortion by surface roughness: Effect upon stability,* AIAA Paper 81–0195, AIAA 19–th Aerospace Sciences Meeting, 1981.

28. C. L. Merkle, K. T-S. Tzou and T. Kubota, *An analytical study of the effect of surface roughness on boundary layer stability,* Dynamics Technology Inc., Report DT-7606-4, 1977.

29. E. Reshotko and A. Tumin, *Investigation of the role of transient growth in roughness induced transition,* AIAA Paper 2002–2850, 32–nd AIAA Fluid Dynamics Conference, St. Louis 2002.

30. J. M. Floryan, J. Szumbarski and Y.Wu, *Stability of flow in a channel with vibrating walls,* Phys. Fluids, **14**, 3927, 2002.

31. S. Leibovich, *The form and dynamics of Langmuir circulation*, Ann. Rev. Fluid Mech., **15**, 391–427, 1983.

32. W. C. R. Phillips, *On the nonlinear instability of strong wavy shear to longitudinal vortices* [in:] *Nonlinear Instability, Chaos and Turbulence*, L. Debnath and D.N. Riahi [Eds.], 251–273, Comp. Mech. Publns, UK 1998.

33. W. R. C. Phillips and Z. Wu, *On the instability of wave-catalysed longitudinal vortices in strong shear*, J. Fluid Mech., **272**, 235–254, 1994.

34. J. M. Floryan, *Centrifugal instability of Couette flow over a wavy wall,* Phys. Fluids, **14**, 312, 2002.

35. J. M. Floryan, *Vortex instability in a converging-diverging channel,* J. Fluid Mech., **482**, 17, 2003.

36. W. Gong, P. A. Taylor and A. Dörnbrack, *Turbulent boundary-layer flow over fixed, aerodynamically rough two-dimensional waves*, J. Fluid Mech., **312**, 1–37, 1996.

37. A. Günther and P. R. von Rohr, *Large-scale structures in a developed flow over a wavy wall*, J. Fluid Mech., **478**, 257–285, 2003.

38. J. Szumbarski and J.M. Floryan, *A direct spectral method for determination of flows over corrugated boundaries*, J. Comp. Phys., **153**, 378–402, 1999.

39. J. M. Floryan, *Two-dimensional instability of flow in a rough channel*, Phys. Fluids, **17**, 044101/8, 2005.

40. H. B. Squire, *On the stability of three-dimensional disturbances of viscous flow between parallel walls*, Proc. Roy. Soc. A, **142**, 621–628, 1933.

41. W. M. Orr, *The stability or instability of the steady motions of a perfect liquid and a viscous liquid,* Proc. R. Irish Acad. A, **27**, 27 and 69, 1907.

42. A. Sommerfeld, *Ein Beitrag zur hydrodynamishen Erklärung der turbulenten Flüssigkeitsbewegung*, In Atti del 4 Congr.Internat. dei Mat., III, Roma, 116, 1908.

43. W. Tollmien, *Ein allgemeines Kriterium der Instabilität laminarer Geschwindigkeitsverteilungen,* Nachr. Wiss. Fachgruppe, Göttingen Math.-phys. Kl. 1, **79**, 1935 (also: *Gene-ral instability criterion of laminar velocity distributions*, [in:] Tech. Memor. Nat. Adv. Comm. Aero. Wash. No. 792, 1936).

44. H. Schlichting, *Berechnung der Anfachung kleiner Störungen bei der Plattenströmung,* ZAMM, 13, 171, 1933.

45. M. Asai and J. M. Floryan, *Experiments on the linear instability of flow in a wavy channel*, European Journal of Mechanics/B Fluids, **25**, 971–986, 2006.

46. J. M. Floryan, *Flow in a channel with simple distributed surface roughness*, Expert Systems in Fluid Dynamics Research Laboratory Report ESFD-1/2003, Department of Mechanical and Materials Engineering, The University of Western Ontario, London, Ontario, N6A 5B9, Canada, 2003.

47. L. N. Trefethen, A. E. Trefethen, S. C. Reddy and T. A. Driscoll, *Hydrodynamic stability without eigenvalues,* Science **261**, 577, 1993.

48. J. Szumbarski and J.M. Floryan, *Transient disturbance growth in a corrugated channel*, J. Fluid Mech., 568, 243–272, 2006.

49. J. M. Floryan, *Stability of shear layers over rough surfaces*, Proceedings of the NATO Specialists Meeting on *Enhancement of NATO Military Flight Performance by Management of Interacting Boundary Layer Transition and Separation*, RTO-MP-AVT-111, Prague, Czech Republic, Oct.4–7, 2004.